The IRAC point response function in the warm Spitzer mission

Joseph L. Hora[*a], Massimo Marengo[b], Rebecca Park[b], Denise Wood[b], William F. Hoffmann[c], Patrick J. Lowrance[d], Sean J. Carey[d], Jason A. Surace[d], Jessica E. Krick[d], William J. Glaccum[d], James G. Ingalls[d], Seppo Laine[d], Giovanni G. Fazio[a], Matthew L. N. Ashby[a], Zhong Wang[a]

[a]Harvard-Smithsonian Center for Astrophysics, 60 Garden St. MS-65, Cambridge, MA 02138-1516 USA; [b]Iowa State University, Dept. of Physics and Astronomy, 12 Physics Hall, Ames, IA 50011-3160 USA; [c]University of Arizona, 949 N. Cherry Ave., Tucson, AZ 85721 USA; [d]Spitzer Science Center, Pasadena, CA USA

ABSTRACT

The Infrared Array Camera (IRAC) is now the only science instrument in operation on the *Spitzer Space Telescope*. The 3.6 and 4.5 μm channels are temperature-stabilized at ~28.7K, and the sensitivity of IRAC is nearly identical to what it was in the cryogenic mission. The instrument point response function (PRF) is a set of values from which one can determine the point spread function (PSF) for a source at any position in the field, and is dependent on the optical characteristics of the telescope and instrument as well as the detector sampling and pixel response. These data are necessary when performing PSF-fitting photometry of sources, for deconvolving an IRAC image, subtracting out a bright source in a field, or for estimating the flux of a source that saturates the detector. Since the telescope and instrument are operating at a higher temperature in the post-cryogenic mission, we re-derive the PRFs for IRAC from measurements obtained after the warm mission temperature set point and detector biases were finalized and compare them to the 3.6 and 4.5 μm PRFs determined during the cryogenic mission to assess any changes.

Keywords: *Spitzer Space Telescope*, IRAC, Infrared camera, point response function, point spread function

1. INTRODUCTION

The *Spitzer Space Telescope*[1] was launched on August 25, 2003, and its cryogenic mission lasted until May 15, 2009, when its supply of liquid helium was exhausted. After a brief recalibration and checkout phase[2], *Spitzer* began its "Warm Mission" operational phase[3] in late July 2009. At its new temperature equilibrium just below 30K, the 3.6 and 4.5 μm channels of the Infrared Array Camera (IRAC)[4], which utilize InSb detectors, can continue to operate at high sensitivity and low dark current[5]. The observatory has been operating nominally and obtaining science data since July 2009, and in April 2012 we passed the milestone of over 1000 days (and counting!) of continuous IRAC operation.

The *Spitzer* point spread function (PSF) is undersampled by IRAC and in the 3.6 and 4.5 μm channels, there is a significant variation in sensitivity across the face of each pixel. In order to account for these effects when performing PSF-fitting photometry or subtracting point sources from images, Point Response Functions (PRFs) were developed for IRAC[6]. A PRF is a table (not an image, though for convenience it is stored as a 2D FITS image file) which combines the information on the PSF, the detector sampling, and the intra-pixel sensitivity variation. By sampling this table at regular intervals corresponding to fractional detector pixel steps, an estimate of the detector point source response can be obtained for a source centered at any given sub-pixel position.

PRFs have several astronomical applications when analyzing *Spitzer*/IRAC data. For example, if one is interested in studying faint companions to bright stars, one can use the PRF to subtract the bright star from the field to better locate and photometer the faint companions[7]. The PRF can also be used to perform PRF-fitting photometry to determine the flux of sources, which is especially useful in crowded fields where many sources overlap and simple aperture photometry is not possible. The PRFs can also be used to perform photometry on sources that are saturated in the IRAC frames by fitting the extended wings of the PSF to a standard star[8]. A well-determined high signal-to-noise PRF is

[*]Email: jhora@cfa.harvard.edu

therefore a useful tool to have available for analyzing IRAC data, and we must derive them for warm *Spitzer* in order to use them with data from the current phase of the mission.

2. CRYOGENIC PRFS

The cryogenic PRFs were derived separately for the core region (within a few arcsec of the center) and the extended PRF (out to a diameter of ~5 arcmin). In order to gain high signal-to-noise out to the edge of the arrays, PRFs were generated from a combination of on-board calibration and science observations of stars with different brightness and joined together to produce extended high dynamic range (HDR) observational PRFs. These PRFs have two main components: a core PRF created by the observations of an unsaturated reference star, and the extended region from observations of a set of bright stars that saturated the IRAC array.

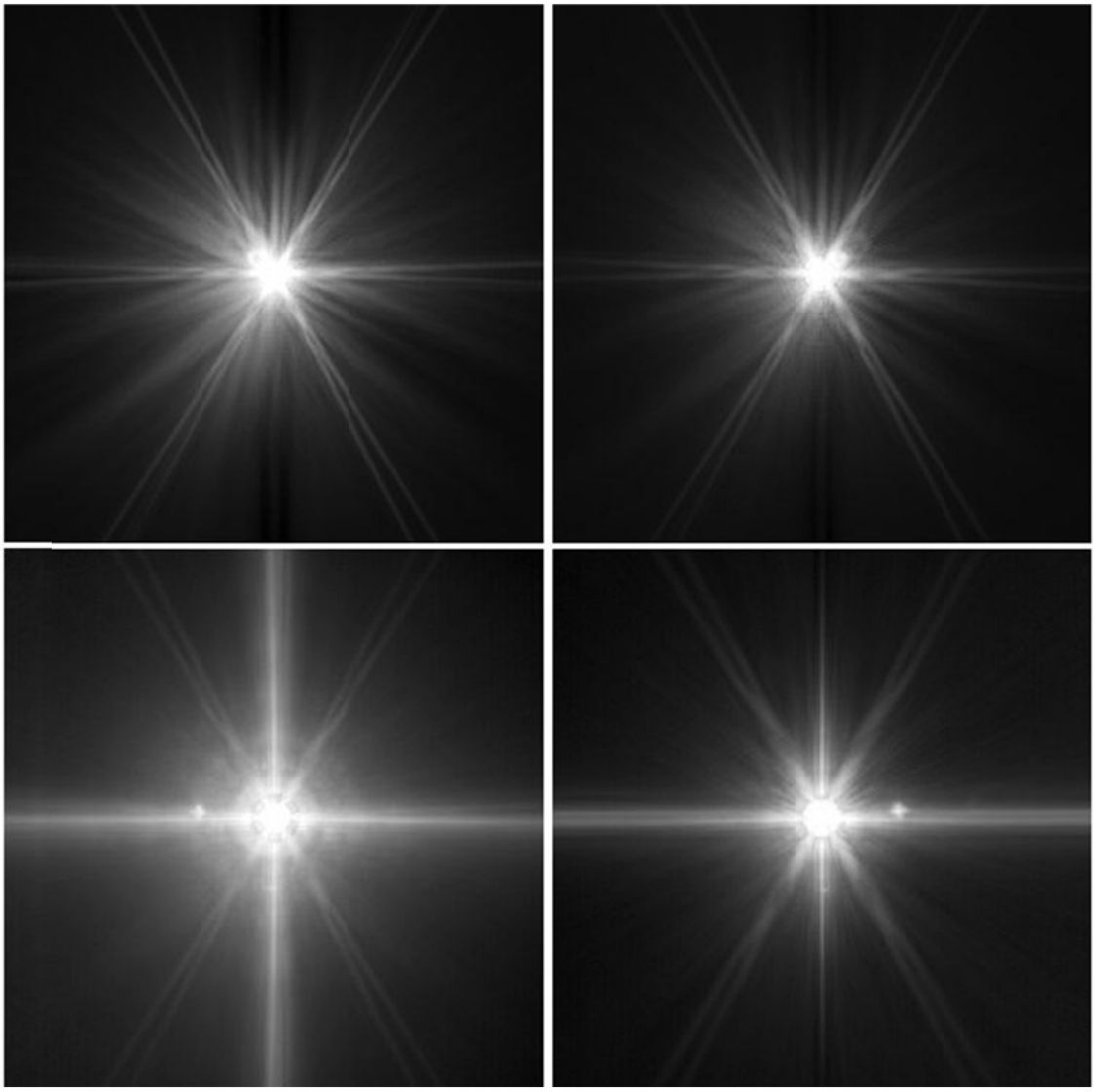

Figure 1. The extended IRAC Cryogenic point response functions (PRFs) for the center of the IRAC arrays. The 3.6 μm PRF is in the upper left, the 4.5 μm in the upper right, the 5.8 μm in the lower left, and 8.0 μm in the lower right box of the figure. The area shown for each image is approximately 5.1 arcmin across. The scaling is logarithmic and adjusted to show the lower-level structure in the images.

To produce the core portion of the PRF, 300 HDR observations of a calibration star were obtained during three separate epochs (and different roll angles). Each observation consisted of short exposures (0.6 sec/1.2 sec) and long exposures (12 sec/30 sec). The PRFs were generated by first combining short-exposure frames and long-exposure frames separately. The images were aligned in each epoch in array coordinates, and the individual epochs were then aligned in reference to the calibration star, allowing us to reject all of the background objects which appeared at different positions in each epoch. The short frames enabled the cores to be constructed without a saturation problem, while the long exposures allowed the construction of a higher signal-to-noise PRF in the wings out to 15 arcseconds. The assembly required the replacement of any saturated areas in the long-exposure frames with unsaturated data from the same pixel area of the short-exposure frames. It also required the replacement of a few pixels in the long-exposure frames by the corresponding pixels in the short-exposure frames to mitigate the non-linear bandwidth effect in channels 3 and 4. The "stitching" of the two components of the PRF was completed using a 1/r masking algorithm requiring a percentage of each frame to be added together over an annulus two IRAC pixels in width just outside the saturated area. Each epoch was treated separately, and then all three epochs were aligned relative only to the PRF star in array coordinates and a median was taken to remove background stars.

Observations of the stars Vega, epsilon Eridani, Fomalhaut, epsilon Indi, Sirius, SAO 17718, and BD +68 1022 were used in the construction of the extended portion of the PRF[7]. Each star was observed with a sequence of 12 sec IRAC full frames, using a 12-point Reuleaux dither pattern with repeats to obtain the required total integration time. The stars were typically observed for 20 – 60 minutes during each epoch. The images were aligned, rescaled to the observation of Vega, and then averaged together with a sigma-clipping algorithm to reject background stars. The core PRFs were aligned and rescaled to the extended PRFs by matching their overlapping area. The alignment was done at best to an accuracy of ~0.1 arcsec. The rescaling was made by forcing the cores to have the same flux density, that of Vega, within a 10 native IRAC pixel radius aperture. The stitching was made using a mask with a smooth 1/r transition zone, 2.4 arcsec wide, between the core (contributing where the extended PRF data were missing due to saturation cutoff), and the extended PRF. The merged extended PRFs were then cropped to a final 5.1 × 5.1 arcmin size, and a pedestal level was removed in order to have a surface brightness as close as possible to zero in the corners of the images.

The cryogenic PRFs are shown in Figure 1. There are several features common to all bands. Near the core, several diffraction rings are visible. There are six diffraction spikes caused by the support vanes of the telescope's secondary mirror. The spikes each split into two parts as they increase in radius from the central source. Ghost images from the IRAC filters appear to the upper left and right of the core in the 3.6 and 4.5 μm images, respectively. Between the diffraction spikes there are more irregular-shaped light and dark bands extending outward from the core. The data for the cryogenic PRFs are available on the *Spitzer* Science Center website[6].

3. WARM MISSION PRFS

In the *Spitzer* warm mission, several of the observatory components have warmer temperatures than during the cryogenic mission. The IRAC body and optics warmed from 1.2 K to ~28 K. The arrays previously operated near 15K and are now stabilized at 28.7 K. The telescope mirrors and supports were in the 5 – 12 K range during the cryogenic mission and are now near 25 K. Based on our knowledge of its materials and properties, the telescope focus and optical performance of IRAC was not expected to change under the warmer conditions in any major way. However, it was anticipated that some features of PRF could change because of potential changes in the alignment of the optics and/or changes in the array characteristics at the warmer temperatures. Therefore we performed a set of measurements in the warm mission to re-derive the PRFs for use in reducing IRAC warm mission data.

3.1 Extended PRF

We used warm mission observations of several stars to derive the extended PRFs in a manner similar to the cryogenic PRFs. The data were from the *Spitzer* program "Search for Planetary Mass Companions of Nearby Young Stars" (Program ID 80071, P.I. M. Marengo). The stars were all observed with an Astronomical Observation Request (AOR) that specified a 12 second full-array frame time, using a 36-point small Reuleaux triangle dither pattern, and 4 repeats at each position, for 144 12s frames on-source at both 3.6 and 4.5 μm at each epoch, with the exception of Altair, that was observed with 6 second frames, 8 repeats. At this frame time, the stars were generally saturated to different levels in the core but this allowed a high S/N measurement of the extended PRF. Each star was observed in two different epochs (and field rotations). The processing steps were the following:

- Create the mosaics for each star, in array coordinates, with 0.24 arcsec/pixel scale;
- mask the saturated/nonlinear area in each mosaic (pixels above 50% full well);
- align all mosaics to the position of a common reference star;
- rescale all aligned mosaics to a common reference star (using the method described above);
- reject any stars that have close companions or other bright sources in the field;
- coadd the aligned/rescaled mosaics together (using outlier rejection to remove background sources from the final PSF).

3.2 Deriving the Core PRF

We derived the core PRF from a set of warm mission standard star observations that were not near saturation at the brightest points. The IRAC standard star BD+67 1044 was observed with a 0.4 sec full array frame time. The observations were taken in order to map the IRAC intra-pixel response function, and they consisted of 10 epochs of 122 frames which used a custom sub-pixel dithering to sample many positions across the pixel near the array center. The data were reduced and combined using the same steps as described above for the extended PRF, except that no pixels in the core of the PRF had to be masked due to saturation or other array effects. In order to construct a composite PRF with both valid core and extended regions, the core PRFs were aligned and rescaled to the extended PRFs by matching their overlapping area using the same method as described above for the cryogenic PRFs.

3.3 The IRAC Warm Mission PRFs

The IRAC warm mission PRFs for the 3.6 and 4.5 μm channels are shown in Figure 3. The images are similar to the ones from the cryogenic mission, with the filter ghost asymmetry visible close to the core and the six diffraction spikes extending from the core and each splitting into two separate spikes at larger distances. The column pulldown effect[9] due to the saturated core of the PRF star on the array is stronger in the warm mission, and therefore the dark vertical band is deeper. Otherwise the images are not visibly different.

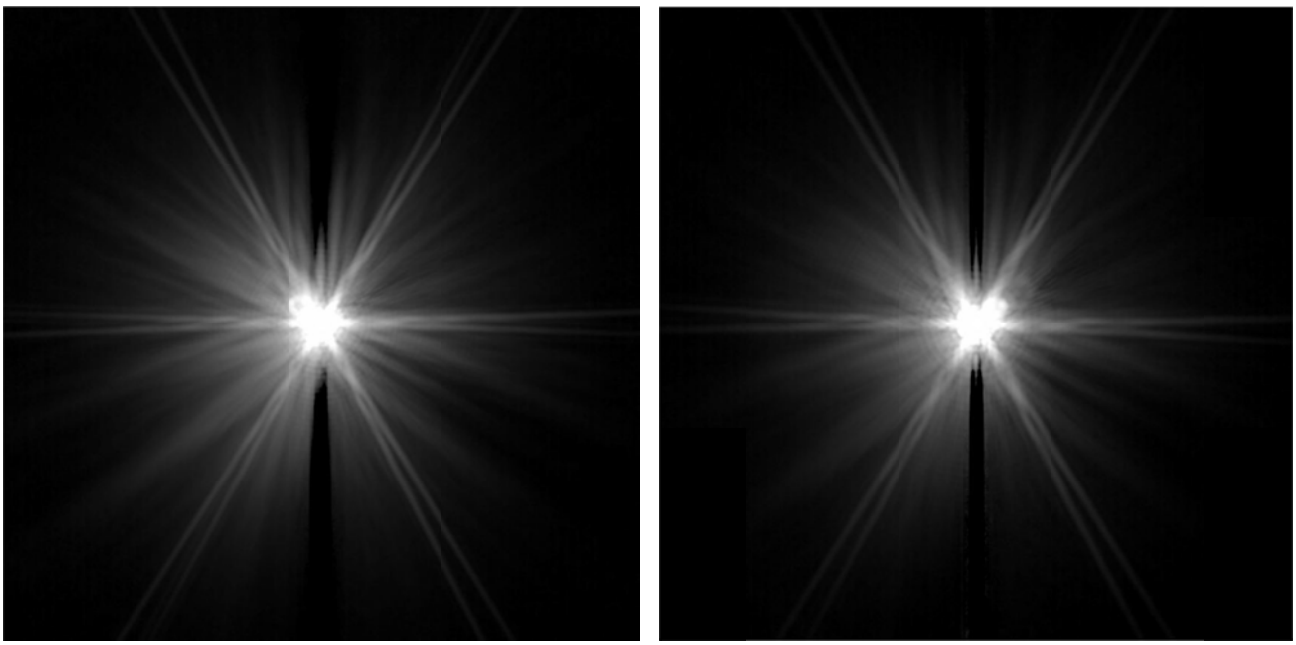

Figure 2. The IRAC warm mission PRFs. The image at the left is the 3.6 μm PRF, and the 4.5 μm PRF is on the right. The images use a logarithmic grayscale to emphasize the low-level emission that extends out to the edge of the ~5×5 arcmin field shown.

4. COMPARISON OF THE CRYOGENIC AND WARM MISSION PRFS

In order to determine the detailed differences between the cryogenic and warm mission PRFs, we can align the images and construct a difference image. The results for the 3.6 μm and 4.5 μm channels are shown in Figure 3, which shows the difference image between the warm and cryogenic PRFs. As expected, the column pulldown and muxbleed effects are different because of the change in the array operating conditions, leading to the black vertical band and light horizontal bands. Some of the differences in banding effects are possibly due to the differences in flux of the stars observed (in the warm mission fainter stars were observed). Since the pulldown is a non-linear effect, scaling the flux in the linear portion of the PRF would result in a mismatch in the pulldown region. The faint vertical lines throughout the image are a result of incomplete dark frame subtraction in the warm mission data. Also seen are slight differences in the diffraction spikes, and dark and light bands that extend to the upper and lower right from the core of the PRF. There are also faint residuals of point sources near the edges of the frame due to incomplete rejection of field stars when the individual observations were combined to form the PRF.

Other differences are visible near the core, where narrow spikes are seen pointing away from the center. There are also wider bands extending out from the core mainly in the regions to the upper and lower right of the center. In the 4.5 μm image, there is a broad positive arc in the upper left quadrant.

Even though the IRAC focus and image quality have not changed significantly compared to the cryogenic mission[5], small changes in alignment, spacing of the optical elements, and the refractive properties of the IRAC lens materials could possibly affect the detailed shape of the PRF. Given the possible optical changes and the differences in the array behavior at the higher temperature and different bias voltages, one should use these new PRFs when analyzing warm mission IRAC data.

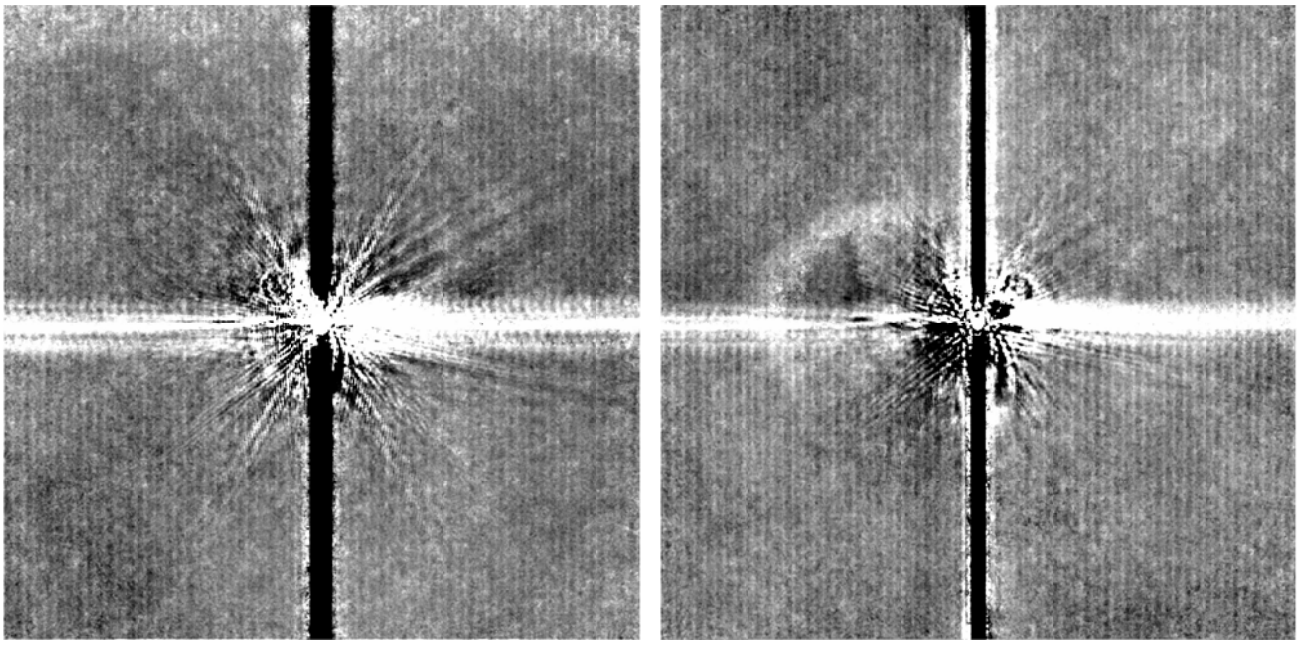

Figure 3. The difference images between the warm mission and cryogenic PRF for channel 1 (3.6 μm) on the left and channel 2 (4.5 μm) on the right. White indicates a higher flux level in the warm mission PRF relative to the cryo PRF. The column pulldown and muxbleed effects are different because of the change in the array operating conditions, leading to the black vertical band and light horizontal bands. The faint vertical lines throughout the image are a result of incomplete dark frame subtraction in the warm mission data. Also seen are slight differences in the diffraction spikes, and dark and light bands that extend to the upper and lower right from the core of the PRF.

ACKNOWLEDGEMENTS

This work is based on observations made with the Spitzer Space Telescope, which is operated by the Jet Propulsion Laboratory, California Institute of Technology under a contract with NASA. Support for this work was provided by NASA through an award issued by JPL/Caltech.

REFERENCES

[1] Werner, M. W. et al., "The Spitzer Space Telescope Mission," ApJS, 154, 1-9 (2004).
[2] Mahoney, W. A., Garcia, L. J., Hunt, J. Jr., McElroy, D. B., Mannings, V., Mittman, D. S., O'Linger, J. C., Sarrel, M., and Scire, E., "Spitzer Warm Mission Transition and Operations", Proc. SPIE 77371W-12 (2010).
[3] Storrie-Lombardi, L. J, & Dodd, S. R. "Downsizing a great observatory: reinventing Spitzer in the warm mission", Proc. SPIE 77370L (2010).
[4] Fazio, G. G. et al., "The Infrared Array Camera (IRAC) for the Spitzer Space Telescope", ApJS, 154, 10-17 (2004).
[5] Carey, S. J., Surace, J. A., Glaccum, W. J., Ingalls, J., Krick, J., Lacy, M., Lowrance, P., Laine, S., O'Linger, J., Stauffer, J. R., Willner, S. P., and Hora, J. L., "Calibration and data quality of warm IRAC", Proc SPIE, 7731, 77310N-1 (2010).
[6] Spitzer Science Center IRAC calibration and analysis files web pages, NASA/IPAC Infrared Science Archive, http://irsa.ipac.caltech.edu/data/SPITZER/docs/irac/calibrationfiles/psfprf/
[7] Marengo, M., Stapelfeldt, K., Werner, M. W., Hora, J. L., Fazio, G. G., Schuster, M. T., Carson, J. C., and Megeath. S. T., "Spitzer/Infrared Array Camera Limits to Planetary Companions of Fomalhaut and epsilon Eridani", ApJ, 700, 1647-1657 (2009).
[8] Marengo, M., Evans, N. R., Barmby, P., Bono, G., Welch, D. L., Romaniello, M., "Galactic Cepheids with Spitzer. I. Leavitt Law and Colors", ApJ, 709, 120-134 (2010).
[9] Hora, J. L., Fazio, G. G., Allen, L. E., Ashby, M. L. N., Barmby, P., Deutsch, L. K., Huang, J. S., et al., "In-flight performance and calibration of the Infrared Array Camera (IRAC) for the Spitzer Space Telescope", SPIE, 5487, 77-92 (2004).